THE ROLE OF DUST FEEDBACK ON THE ORBIT-SPIN COUPLING HYPOTHESIS OF GLOBAL DUST STORM FORMATION ON MARS

M. A. Mischna, J. H Shirley, *Jet Propulsion Laboratory, California Institute of Technology, Pasadena, CA, USA (michael.a.mischna@jpl.nasa.gov),* **C. E. Newman**, *Aeolis Research, Pasadena, CA, USA*

Introduction:

We have modified the MarsWRF general circulation model (GCM) to include the modifying effects of a coupling term acceleration (CTA) on atmospheric circulation. The CTA is a small horizontal acceleration (~10^{-5} ms^{-2}) that is obtained from derivation of the momentum equation in a barycentric, or inertial, reference frame, and which couples the time rate of change of planetary orbital angular momentum to the angular velocity of Mars' rotation about its spin axis [1]. A remarkable relationship between the CTA and the presence or absence of global dust storms (GDSs) on Mars has been observed [2], suggesting that the CTA may be a regulating factor in GDS initiation, and might be used as a way of forecasting future GDS activity.

Prior Work:

Initial modeling studies with MarsWRF were designed to understand the role of the CTA on atmospheric circulation, and were greatly simplified by design. Preliminary investigations assumed a dust-free atmosphere (i.e. dust was distributed in a prescribed fashion and was not radiatively active in the model) [3]. Because of the novel aspect of the CTA hypothesis, a purposeful decision was made to highlight the role of the CTA on atmospheric circulation by removing potential complications due to various diabatic processes such as atmospheric dust heating, and corresponding radiative feedbacks.

Briefly, the CTA may be represented as shown in Eq. 1

$$CTA = -c\left(\dot{L} \times \omega_{\alpha}\right) \times r \qquad (1)$$

where $\dot{L}$ represents the time rate of change of planetary orbital angular momentum, ω_{α} represents the angular velocity of Mars' rotation, and r indicates a point in the martian atmosphere at which the CTA is to be calculated. The remaining term, c, represents a coupling 'efficiency' factor between the orbital and rotational reservoirs, and is constrained by observations to be very small. For our dust-free atmospheric simulations [3], we determined that a value of c of $5\text{x}10^{-13}$ yielded an appropriately detectible (but not overwhelming) effect by the CTA; however, as noted, the chosen value for c was, and is, specific only to the particular implementation of MarsWRF (i.e. dust-free), and will likely vary as different model parameters are adjusted.

Telescopic and orbital observations of Mars are used to establish the occurrence of past GDS activity [4]. In 21 past Mars years (MY) we have sufficient evidence to confirm either the presence or absence of GDS activity on Mars. A list of these years is found in Table 1. Of these 21 years, eight had what is referred to in [3] as 'positive' polarity during the perihelion season, indicating that the CTA forcing function ($\dot{L}$) was at or near its positive peak during perihelion (indicating an increase with time of Mars' orbital angular momentum during this season). Of these eight years, seven experienced a GDS. The lone exception, MY 27, had an exceptionally small magnitude of $\dot{L}$. Six of the 21 overall Mars years had 'negative' polarity, with $\dot{L}$ at or near its negative peak near perihelion. In two of these years a GDS was observed, both of which (MY 12 and 25) were extremely early season storms, occurring closer to equinox than perihelion. Finally, of the remaining seven Mars years with 'transitional' polarity ($\dot{L}$ at or near zero at perihelion), none had a GDS. At the time of this writing, it is approaching perihelion in MY 33. Based on comparisons to MarsWRF simulations for these prior Mars years, a forecast in [3] suggests that a GDS might be expected this Mars year. We shall be able to comment on its (non-) occurrence at the workshop.

Whether or not the GDS prediction for MY 33 is correct, our simplified model scheme does not capture many of the subtleties of circulation that arise from the presence of atmospheric dust. Consequently, we must consider the impact of dust behavior on the atmospheric circulation to ensure the greatest model fidelity. Following our prior approach of taking simple, discrete steps for our CTA analysis, we continue to incrementally add to the MarsWRF model, first by including radiatively active (but prescribed) dust to the atmosphere. These results invoke a time-evolving distribution representative of past Mars years, but do not require any active lifting, settling or surface sources. These latter behaviors are tackled, in turn, in subsequent investigations, which consider interactive dust, and limited surface sources, respectively. We show high-level findings of these investigations presently.

Radiatively Active Dust:

To advance the sophistication of the GCM, we have performed a series of tests that include radiatively active (but not interactive) dust, using a simple distribution from the Laboratoire de Météorologie Dynamique (LMD) Mars GCM [5], incorporated into the Mars Climate Database [6] and chosen to fit most of the thermal profiles observed during the Mars Global Surveyor mission. A comparison of an otherwise identical simulation with or

without dust is shown in Figure 1. The overturning circulation in the dust-free scenario is comparatively shallow in comparison to a simulation including dust, due to the absence of radiative heating effects of dust in the dust-free model run, which will 'inflate' the warmer atmosphere. This is a clear indication that the dust-free atmosphere is a gross simplification of what we should expect in the real martian atmosphere.

A series of tests (not shown) have been performed with radiatively active dust, over a range of putative efficiency factors, and are compared to similar tests performed for dust-free atmospheres. These comparisons do show an influence by atmospheric dust, even in the absence of the CTA. Interestingly, the presence of dust in the atmosphere appears to reduce global mean wind magnitude and, correspondingly, modifies the distribution of surface stresses (Figure 2), with an overall reduction across most of the surface.

Although limited, dust opacity data is also available from TES limb observations for MY 24-27, covering both 'clear' atmospheres as well as the MY 25 GDS. Future investigations will use these data to refine our radiatively active dust investigations.

Interactive Dust:

We next address interactive dust, having run the MarsWRF GCM with parameterized dust lifting following the approach used in [7]. Briefly, two separate parameterizations are used to raise atmospheric dust, one for dust devil lifting and one for wind stress lifting. The former is responsible for 'background' dustiness, and is tuned to match globally averaged T_{15} temperatures in the low and mid-latitudes (T_{15} temperatures are a vertically weighted temperature that mimics observations taken by the Viking IRTM instrument in the 15 μm band). Once properly tuned to achieve proper seasonal background dustiness, wind stress lifting is added, which consists of a parameter to scale the amount of lifted dust, and a threshold wind stress (set, in our model, to 0.036 Pa), above which surface dust can be lifted into the atmosphere. Proper tuning of these parameters allows for the occurrence of GDS (defined as producing sustained global T_{15} temperatures >210 K) in the appropriate season and of the appropriate magnitude. From this, we can assess the added influence of the CTA.

Control Runs: Figure 3 shows MarsWRF results for a 28-year simulation from MY 8 to MY 35 that includes interactive dust, but does not include the CTA. This serves as a 'control' run for interactive dust comparisons (the four panels are identically structured, each illustrating seven consecutive years, for clarity). The stark rise in T_{15} surface temperature around southern summer (L_s=250°) is highly repeatable year after year, and is seen in all model years with only slight variation. This shows the repeatability of MarsWRF behavior, and is specific to the choice of tuning parameter(s) which initiate dust storm activity at approximately the right season. However, the annual occurrence of GDS is clearly not representative of the observed behavior of the martian atmosphere, which sees only occasional GDS activity.

CTA Runs: By comparison, Figure 4 shows a 28-year simulation which includes the CTA. Two important things are observed in these runs in contrast to Figure 3. First, the timing of storm initiation is more highly variable, which reflects the influence of the variable phasing of the CTA each year. Second, there is significantly greater variability in the magnitude of the established storm, ranging from strong GDS activity (e.g. MY 12, 15, 25) to more modest regional-type storms with T_{15} <210 K (e.g. MY 14, 18, 27).

The results of our preliminary interactive dust simulations are encouraging, albeit inconclusive. Perhaps the most satisfying behavior of the CTA runs is the large interannual variability that more accurately mirrors observations. Furthermore, we note that some of the warmest T_{15} temperatures occur in years in which GDSs were actually observed (e.g. MY 12, 15, 25). We are continuing to explore the interplay between CTA and the dust lifting parameters as a means of refining this type of observation.

Surface Dust Reservoirs:

Thus far, we have assumed an infinite source of dust at the surface, which allows dust to be endlessly lifted when conditions allow (i.e. surface stresses exceed the chosen surface stress threshold for lifting). This is assuredly inaccurate, as dust is a limiting resource for the initiation and growth of GDS. We have evidence of albedo changes following GDS which suggest dust is scoured from certain primary sites and redistributed elsewhere [8]; however, with infinite surface sources, the majority of atmospheric dust will be derived from just a few select sites—those with the greatest surface stresses, in contrast to observations.

We may mitigate this issue by considering dust on the surface to be a finite resource. Once a particular source region is exhausted, subsequent dust lifting must occur from other secondary or tertiary locations not yet depleted. Additionally, finite dust reservoirs require us to consider the role of dust sedimentation in our model. With infinite reservoirs, dust sedimentation may be ignored, but with a finite source, replenishment of specific regions, and the timescale on which such replenishment occurs plays a critical role in GDS formation. Simulations with finite dust sources are ongoing and are discussed in [9].

Summary:

We are continuing our assessment of the potential role the CTA may have on atmospheric circula-

tion and on the establishment of GDS on Mars. Prior work set aside the role of atmospheric dust as a simplifying measure, and revealed a remarkable correspondence between the CTA and GDS activity. Presently, we are assessing the feedback-like role of atmospheric dust itself on continued growth and sustenance of GDS. We have proceeded in a stepwise fashion, introducing incremental changes in the model so as to characterize the key components of the dust system. Radiatively active, but non-interactive atmospheric dust shows interesting behavior in our simulations, and points to the dependence of the coupling 'efficiency' factor on the atmospheric state. We suggest modifications to our prior value of '*c*' for a model with radiatively active dust.

With additional complexity, we can simulate interactive dust lifting and sedimentation, which adds an additional fidelity to our model. Interactive dust simulations with CTA show better interannual variability than without. Finally, by incorporating limited dust reservoirs on the surface, we have begun to develop a relatively realistic scenario that requires us to convolve both the CTA and dust availability into our model of GDS initiation. This illustrates the heretofore ignored (by us) fact that, regardless of the efficacy with which dust may be lifted, given the magnitude of the local surface stress, if there is no dust to lift, nothing will happen. Future studies will examine the nexus of these two components to identify potentially important lifting sites as well as refinements to putative stress lifting thresholds and coupling efficiencies.

References: [1] Shirley, J.H., https://arxiv.org/abs/1605.02707 [2] Shirley, J.H., Icarus 252, 128-144, 2015 [3] Mischna, M.A. and J.H. Shirley, https://arxiv.org/abs/1602.09137 [4] Zurek, R.W. and L.J. Martin, J. Geophys. Res. 98, 3247-3259, 1993 [5] Forget, F. et al., J. Geophys. Res. 104, 24155-24175, 1999 [6] Millour, E. et al., EPSC 2015-438, 2015 [7] Newman, C.E. and M.I. Richardson, Icarus 257, 47-87, 2015 [8] Szwast, M.A. et al., J. Geophys. Res. 111, 2006. [9] Newman, C.E. et al., 6th MAMOW (*this workshop*)

Acknowledgements: This work was performed at the Jet Propulsion Laboratory, California Institute of Technology, under a contract from NASA. Funding from NASA's Solar System Workings Program is gratefully acknowledged. Government sponsorship acknowledged.

Table 1:List of all years with known presence or absence of GDS activity, and seasonal start date of all GDS.

GDS Years	
Mars Year [Earth Year]	GDS Start Date (L_s)
-16 [1924]	310
1 [1956]	249
9 [1971]	260
10 [1973]	300
12 [1977]	204, 268
15 [1982]	208
21 [1994]	254
25 [2001]	185
28 [2007]	262

Non-GDS Years
Mars Year [Earth Year]
-8 [1939]
11 [1975]
17 [1986]
18 [1988]
23 [1998]
24 [2000]
26 [2003]
27 [2005]
29 [2009]
30 [2011]
31 [2013]
32 [2015]

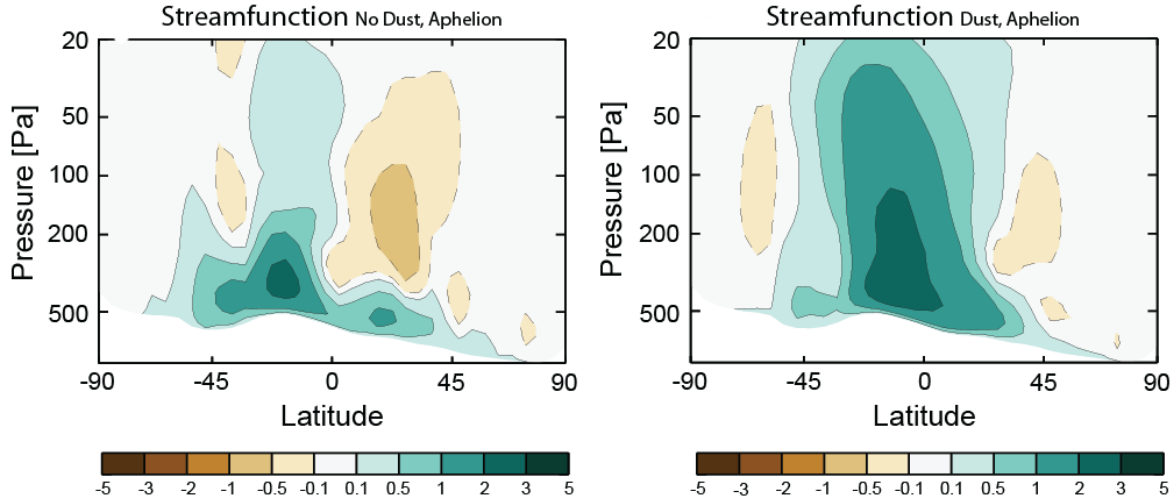

Figure 1: Zonal mean meridional mass streamfunction during aphelion season (averaged over L_s=70-90°) with (left) no radiatively active dust and (right) radiatively active dust. Streamfunction units are 10^9 kg/s. Positive values indicate counterclockwise circulation in this perspective.

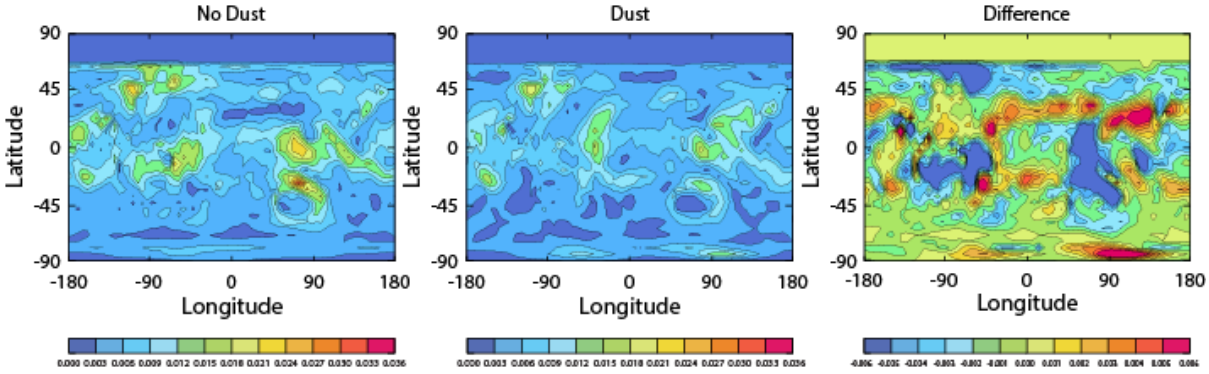

Figure 2: Model-derived daytime surface stresses during perihelion (L_s=250-270°) for (left) simulation with no radiatively active dust, and (middle) radiatively active prescribed dust. (Right) Difference between the two simulations (dust minus no dust). Homogeneous band poleward of ~60°N is in northern winter, where there are no daytime hours.

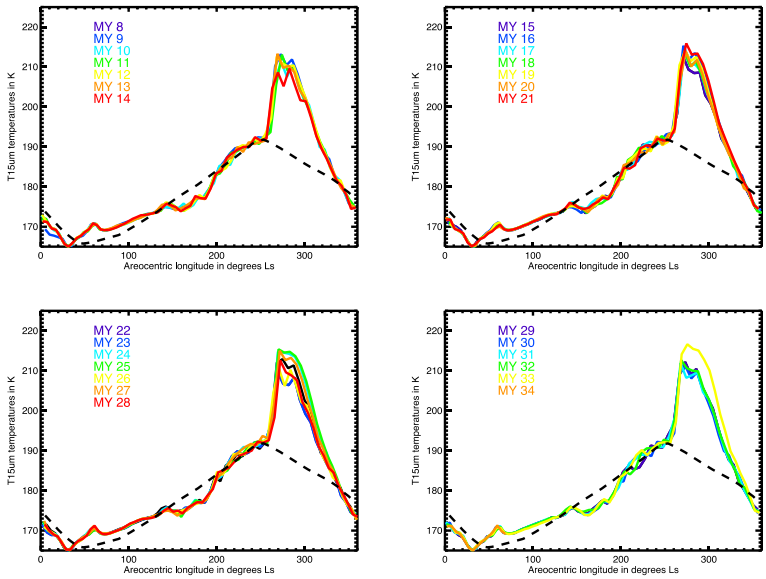

Figure 3: T_{15} temperature as a function of season for MY 8-34 with parameterized wind stress and dust devil lifting and radiatively active dust using a wind stress lifting parameter, α_N, of 4×10^{-5} and excluding CTA accelerations. Dashed line

represents mean background T_{15} temperature observed in years without a GDS.

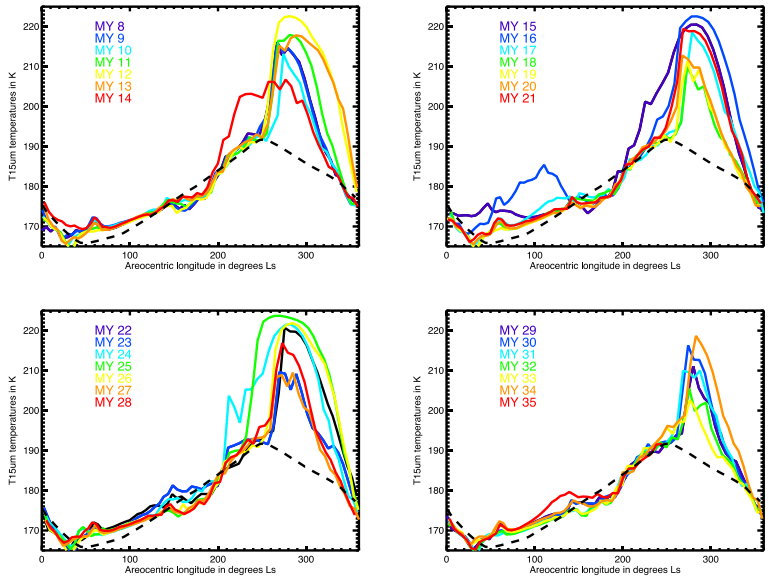

Figure 4: Same as Figure 2 but with CTA accelerations.